EasyChair Preprint

№ 13838

Feasibility Study of the Flat Joint Method Using High-Tension Bolt Friction Joints in Light-Gauge Steel Structures and Fundamental Study on Resistant Mechanism

Nagi Hamada, Jihang Feng, Takumi Ito, Natsuhiko Sakiyama, Katsunori Onishi, Kenjiro Mori and Rikako Hotta

July 6, 2024

Feasibility Study of Flat Joint Method Using High-Tension Bolt Friction Joints in Light-gauge Steel Structures and Fundamental Study on Resistant Mechanism

Nagi Hamada[1], Jihang Feng[1], Takumi Ito[1], Natsuhiko Sakiyama[1], Katsunori Onishi[2], Kenjiro Mori[3], Rikako Hotta[4].

[1] Dept. of Architecture, Tokyo University of Science, Tokyo, Japan
[2] Building System Design Co. Ltd, Tokyo, Japan
[3] Dept. of Architecture, Hiroshima Institute of Technology, Hiroshima, Japan
[4] Nippon Steel Metal Production Co. Ltd, Tokyo, Japan

Mail Adress: naginagi20010724@outlook.jp

Abstract. Recently, light-gauge steel structures that can reduce the amount of steel compared to heavy steel structures have attracted more attention. However, there are no detailed guidelines for designing joints in light-gauge steel structures in Japan. To provide the rigid joints in light-gauge steel structures, processing and construction gets complicated, and projections on the flange by jointing with bolts can interfere with the floor slab and finishing materials. In this context, this study proposes the flat joint method, a joint method that has no projections on the flange by frictional bolted jointing at only the beam web and aims to develop a rigid joint without welding. The flat joint method has a frictional steel plate to connect, which transfers stress on the beam to the other one through frictional force. Therefore, the flat joint method follows the mechanical principles of the joint function.

A tensile test of the flat beam joint was conducted to reveal the fundamental mechanical properties. It was expected that the flat joint will be a complex stress transfer mechanism for the distribution of cross-sectional stress under bending forces, because of the contact and arrangement of plate and joint elements, and the mechanical relationships due to bearing stress and friction. Additionally, we analyzed findings from this tensile test in detail by using the finite element analysis method. From the results of the tensile test and finite element analysis, evaluation methods for mechanical properties of the flat joint under tensile force were determined.

Keywords: Light-gauge Steel Structure, Flat Joint, Friction bolt joint, Tensile Test, FEA

1 Introduction

Japan has an extensive history of steel structures. More recently light-gauge steel structures that can reduce the amount of steel compared to heavy steel structures have attracted more attention. In the future, it is expected to apply light-gauge steel structures to large scale buildings by combining them with heavy steel structures and to use light-gauge steel structures as hybrid structures with timber [1]. However, there are no detailed guidelines for designing joints in light-gauge steel structures in the Guidelines for the Design and Construction of Light-gauge Steel Structures (transaction of AIJ) [2]. Therefore, most construction companies usually use their own design methods. In addition, when aiming for rigid joints in light-gauge steel structures, processing and construction get complicated, and projections on the flange by bolted joints can interfere with floor slab and finishing materials.

In this context, this study proposed the flat joint method, a joint method that has no projections on the flange by friction jointing at the only the beam web and aims for rigid joint behaviour without welding. Diagrams of the flat joint in light-gauge steel structures are shown in Fig.1. This method consists of high-tension bolts and frictional steel plates to connect with the other structural members, which transfers stress on one beam to the other one through the frictional force. Therefore, the flat joint method follows the mechanical principles of the joint function. Furthermore, it makes construction speedy owing to no welding process and slab and finishing materials construction easy because of no projections on the beam flange. Double beams will be used as a group to generate a symmetrical I section and so avoid eccentric stress that a single channel would develop, as well as symmetric force transfer through the connection.

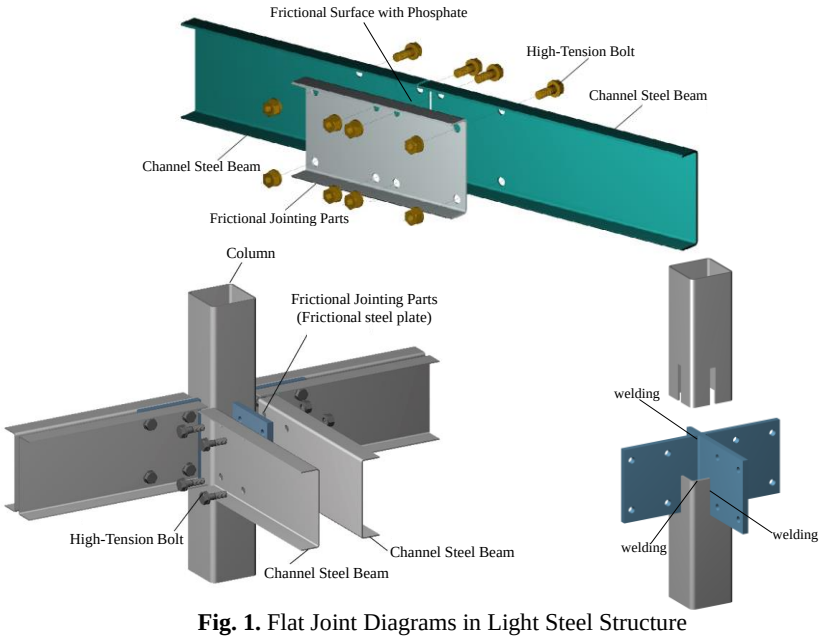

Fig. 1. Flat Joint Diagrams in Light Steel Structure

Figs. 2a and 2b show the theoretical mechanical behavior subjected to tensile force and bending moment. As usual, most of the bending stress is borne by the flange. However, in the flat joint method, stress on the flange is not transmitted directly to the connection because the beam flange is not directly jointed to the jointing parts. Thus, as shown in Fig.2, stress on the flange is transmitted as shear stress to the section between the flange and bolt holes. For this theory, distance between bolts (L_s) influences transmitting stress on the flange.

A tensile test of the flat beam joint was conducted to reveal the basic mechanical properties of the flat joint method, because it was expected of the flat joint to be a complex stress transfer mechanism for the distribution of cross-sectional stress under bending forces. This is due to the contact and arrangement of plate and joint elements, and the mechanical relationships due to the bearing stress and friction.

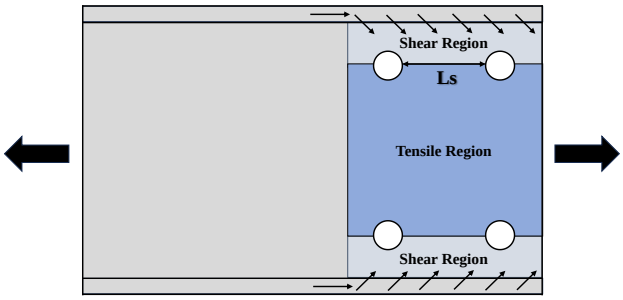

Fig. 2a. Mechanical Behavior under Tensile Force

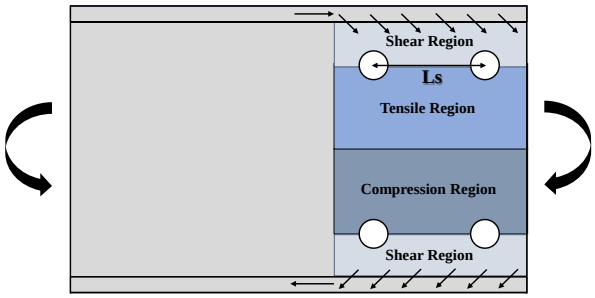

Fig. 2b. Mechanical Behavior under Bending Force

2 Experimental Investigation of Basic Resistant Mechanism

2.1 Test Specimen of the Flat Beam Joint for a Tensile Test

Both beams and jointing parts are made of corrosion-resistant hot dip Zinc-Aluminum-Magnesium alloy (ZAM), which has a superior rust-prevention performance to zinc only coating and is easier to process. All the test specimens were manufactured by the cold-forming method. High-strength TC bolts were used for jointing, which are easy to tighten with an electric wrench. The material test was conducted in accordance with

JISZ2241, to determine the mechanical properties of materials used in the beam and jointing parts. The mechanical properties of the ZAM steel plate obtained in the material test results are summarized in Table 1 below. The specimens were classified as A and B.

Table. 1. Mechanical Properties of Material Used in Beam and Jointing Parts

Classif-ication	Test Piece Label	Steel type	Yield Stress σ_y[N/㎟]	Maxmum Strength σ_u[N/㎟]	Young's Modulus E[kN/㎟]
A	PL-3.2	ZAM	350	440	207
	PL-4.5		339	423	207
B	PL-3.2	ZAM	334	440	185
	PL-4.5		292	407	197

The theoretical scheme to transfer stress on the flange properly to the beam web is shown in Eq (1).

$$L_s \geq \sqrt{3} \cdot B \tag{1}$$

L_s : distance between bolts [mm], B : width of beam [mm]

According to this scheme, the minimum distance between bolts to transfer stress on the flange appropriately is 86.6mm. Therefore, the distance between bolts was focused on and considered as experimental parameters. Also, the end distance and thickness of jointing parts were set as experimental parameters to reveal what factors affect the resistant mechanism. The list of specimens is summarized in Table 2 below, and test specimen details are shown in Fig. 3.

Table. 2. List of Specimens

classi-fication	Identification Label （e-t-Ls)			
A	22-3.2-80	22-4.5-80	22-3.2-120	22-4.5-120
B	22-3.2-40	22-4.5-40	28-3.2-80	28-4.5-80
	28-3.2-90	28-4.5-90	28-3.2-120	28-4.5-120

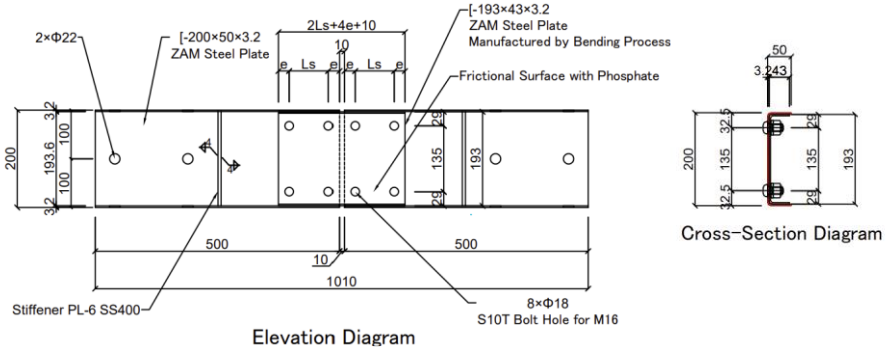

Fig. 3. Test Specimen details (unit: mm)

2.2 Loading and Measuring Methods

To reveal the basic mechanical properties of the flat joint method, A static tensile test was conducted until observing the failure mode. The diagram of the test setup is shown in Fig.4a.

2000kN universal testing machine was used and both sides of the web and flange were grabbed with the jig with M22 high-strength bolts. To prevent the fixed end from yielding, it was strengthened with welded steel plates. Strain gauges were pasted on the jointing parts web and the beam web and flange to clarify the stress transmission paths, as shown in Fig. 5. Displacement between stiffeners was measured by a displacement transducer and measure type transducer. Displacement between crossheads is measured in the same way. Please note that the measuring methods are different for classifications A and B.

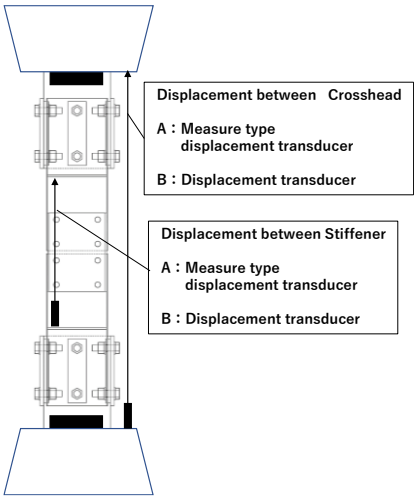

Fig. 4a. Test Setup Diagram

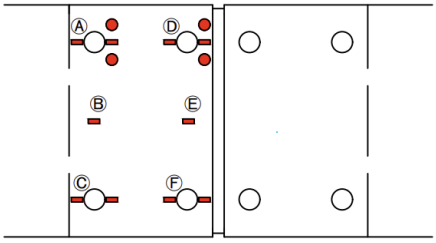

Fig. 5a. Beam Web Strain Gauges

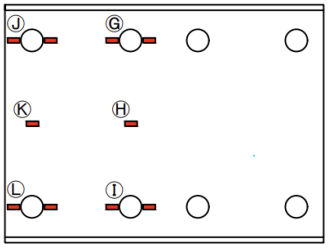

Fig. 5b. Jointing Parts Web Strain Gauges

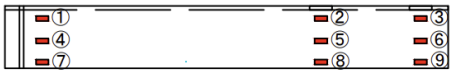

Fig. 5c. Beam Flange Strain Gauges

2.3 Experimental results of tensile tests

In this experiment, yielding, frictional surface slipping and end opening fracture were observed. On account of the dispersion of frictional strength, 5 patterns were observed in the collapse process, and Table.3 shows the collapse process. Data of the elastic limit stress, yield stress, frictional strength, effective cross section yield and maximum

strength that are obtained in this tensile test are shown in Table.4. P- δ curves that were classified based on the collapse process are shown in Fig.6. Strain distribution diagrams at yield strength that were measured by strain gauges are shown in Fig.7.

By defining the proportional limit (P_y) in P- δ curves as the point at which gradient changes, the slope of the line passing through the two points at 0.5 and 0.8 times proportional limit was defined as an initial stiffness. The elastic limit strength is the point at which any strain gauges reach the yield strain, or the parts where triaxial gauges were pasted on follow Von-Mises's yield rules. The frictional strength was defined as the point at which a slipping sound was observed during the test, and the load was dropped in P- δ curve.

In all specimens, the elastic limit strength was determined by mainly local yield that occurred in the near free end side bolt, caused by the transmission of stress from the flange and stress concentration at the bolt tightening area. Also, a decrease of stiffness was not observed at the elastic limit strength. Additionally, the elastic limit strength was not affected by the distance between bolts (L_s).

As regards frictional strength, we confirmed the dispersion of coefficient of friction based on the tightening torque. This dispersion in the coefficient of friction originates from the difference in manufacturing time of specimens classified by A and B.

The proportional limit point in P- δ curves was defined as yield strength(P_y) and it was revealed that yield strength was determined by frictional surface slipping or effective section yield. In the case of effective section yield, stress-bearing and non-stress-bearing cross sections were observed at beam web (Fig.7a). To clarify the effects of bolt distance (L_s) on the effective section on the flange, the 22-3.2-80 was compared with the 22-3.2-40 as shown in Fig.7b. Consequently, differences in the effective cross section on the flange were observed between the two specimens. These differences are ascribed to the size of shear stiffness at the bolt section between bolts (L_s).

The mechanical behavior model is shown in Fig.8. As for the criteria of transmitting the flange stress based on the results of this tensile test, the equation was shown in Eq (2) by comparing the shearing strength of the area where the flange stress is transmitted with the flange yield stress.

$$L_s \geq \sqrt{3} \cdot B - e \tag{2}$$

e: end distance [mm]

When the distance between bolts satisfies Eq (2), the shear stiffness to transmit flange stress is equipped.

The ultimate state of 22-3.2-80 and 22-3.2-40 were shown in Fig.9. The maximum strength was determined by the frictional surface slipping or end opening fracture and bearing failure. In specimen of L_s=40mm, maximum strength tended to be lower than the other specimens because shear failures occurred between the force side bolts and free edge. As for the others, end opening fractures occurred at force side bolt, and bearing failures did at the free edge side bolts.

Table. 3. Results of Collapse Process

Collaps Process	1	2	3	4	5
	$P_e \rightarrow P_{ey} \rightarrow P_f \rightarrow P_u$	$P_e \rightarrow P_f \rightarrow P_{ey} \rightarrow P_u$	$P_e \rightarrow P_{ey} \rightarrow P_f > P_u$	$P_f \rightarrow P_e \rightarrow P_u$	$P_f \rightarrow P_e \rightarrow P_{ey} \rightarrow P_u$

Table. 4. Summary of the Tensile Test Results

Classif-ication	Specimen Label	Initial Stiffness K[kN/mm]	Elastic Limit Strength P_e[kN]	Frictional Strength P_f[kN]	Effective Cross section Yield Strength P_{ey}[kN]	Yield Strength P_y[kN]	Maximum Strength P_u[kN]	Collaps Process
A	22-3.2-8	85	252	422	400	400	429	1
	22-4.5-8	83	89	374	374	374	447	2
	22-3.2-12	118	265	393	393	393	414	2
	22-4.5-12	128	231	435	404	404	455	1
B	22-3.2-40	155	284	332	317	317	332	3
	22-4.5-40	135	92	308	308	308	339	2
	28-3.2-80	222	373	362	-	362	426	4
	28-4.5-80	301	308	320	360	320	453	5
	28-3.2-90	119	286	246	287	246	389	5
	28-4.5-90	208	239	263	310	263	396	5
	28-3.2-120	386	243	244	404	244	407	5
	28-4.5-120	238	326	351	351	351	443	2

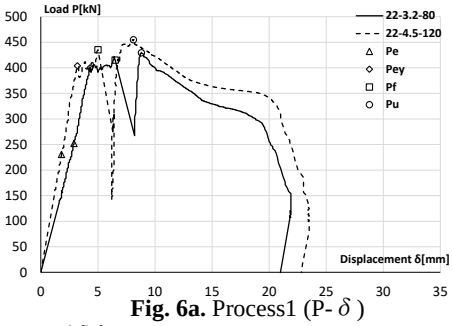

Fig. 6a. Process1 (P- δ)

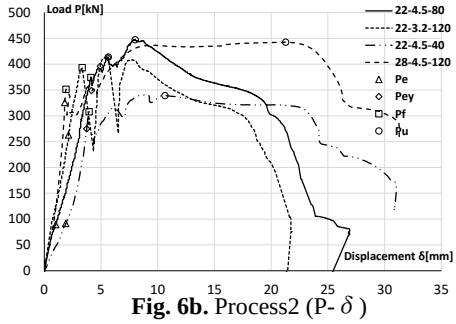

Fig. 6b. Process2 (P- δ)

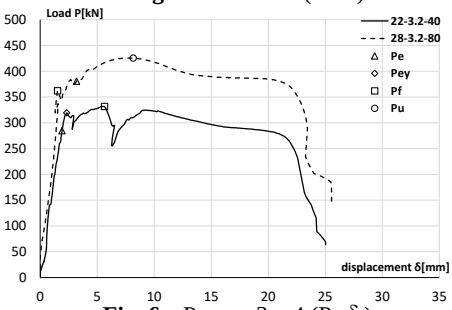

Fig. 6c. Process3・4 (P- δ)

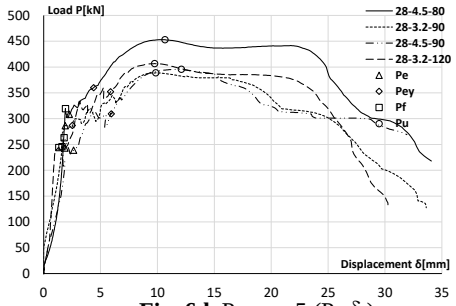

Fig. 6d. Process5 (P- δ)

Fig. 6. P- δ Curves classified based on the collapse process

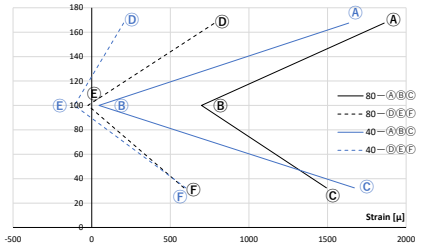

Fig. 7a. Beam Web

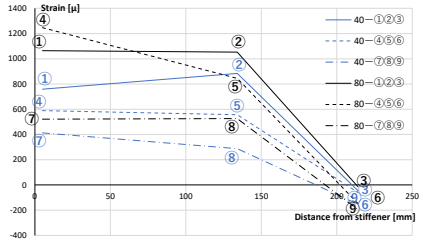

Fig. 7b. Beam Flange

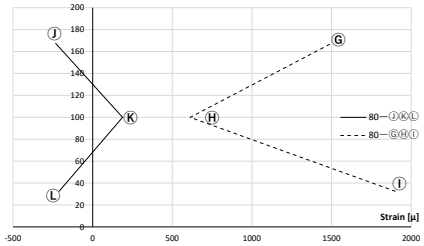

Fig. 7c. Jointing Parts Web

Fig. 7. Strain distribution diagram at yield strength

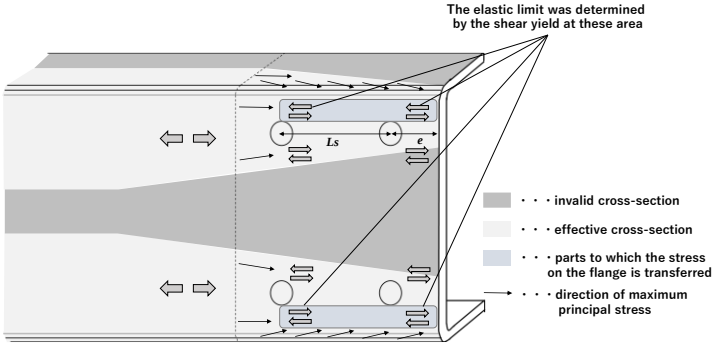

Fig. 8. Mechanical behavior model based on the tensile test results

Fig. 9a. 22-3.2-80

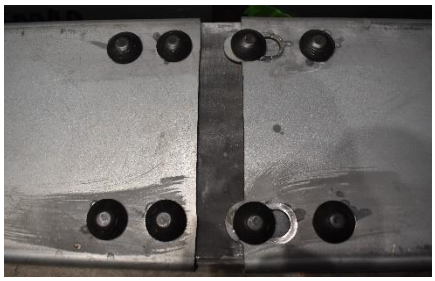

Fig. 9b. 22-3.2-40

Fig. 9. Figure of ultimate state of the specimens

3 Analytical Study Using Finite Element Analysis Method

3.1 Outline of finite element analysis

Using the results of the material test, the mechanical properties of the material used in FEA was defined as shown in Fig.9. The yield rule of ZAM steel is based on Von Mises's yield rules. The elements of the model used 8 node hexahedron elements and 4-node tetrahedron elements in bolts. In the tensile test, different tendencies were observed between specimens of L_s=40mm and the others. Therefore, we analyzed 22-3.2-80 and 22-3.2-40.

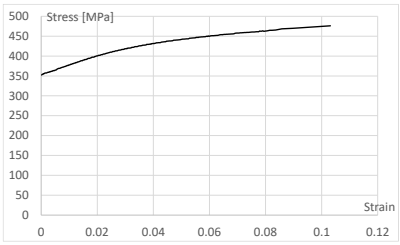

Fig. 9. Mechanical property of the ZAM steel

3.2 Results from FEA

It was confirmed that the elastic limit was determined by the shear yield in both specimens as shown in Figs.10a and 10b.

As for the effective cross-section, Figs.7a and 7b show that stress is gradually transferred to the jointing parts through the frictional force. Thus, this study investigates stress distributions in the cross-section which are all stress is transmitted as shown in Fig.11. The diagrams of cross-sectional Von Mises Stress distributions at the yield strength are shown in Fig.12a and Fig.12b. From these results, the reduction factors of the beam flange and web were determined, and the calculated reduction factors based on Eq (3a) and Eq (3b) are shown in Table 5 below.

$$\beta_f = \frac{1}{B \cdot \sigma_y} \cdot \int_0^B \sigma_{eq}(x)dx \tag{3a}$$

$$\beta_w = \frac{1}{d \cdot \sigma_y} \cdot \int_0^d \sigma_{eq}(x)dx \tag{3b}$$

B: width of beam [mm], d: depth of beam, σ_y: yield stress [MPa],
$\sigma_{eq}(x)$: equivalent Von Mises stress at x [MPa], β: reduction factor

There was no difference in the effective cross section of the beam web between the 22-3.2-40 and 22-3.3-80, and it was confirmed that 57% web cross section was found to be effective. In the flange, 30% of the cross section was effective for the 22-3.2-40 and 46% of that was effective for the 22-3.2-80.

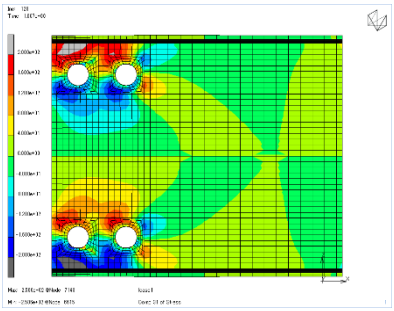

Fig. 10a. 22-3.2-40

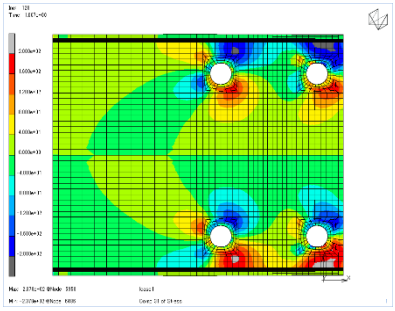

Fig. 10b. 22-3.2-80

Fig. 10. Contour diagram of the τ_{zx} distribution

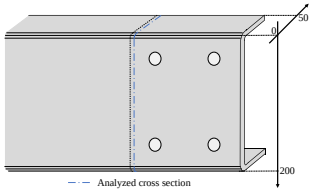

Fig. 11. Target cross section

Table. 5. Reduction factor

Specimen Name		22-3.2-40	22-3.2-80
β	Flange	0.30	0.46
	Web	0.57	

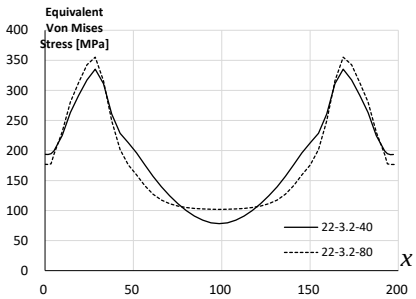

Fig. 12a. Web

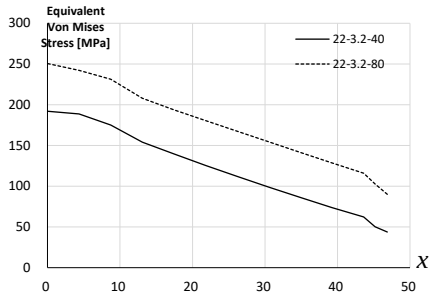

Fig. 12b. Flange

Fig. 12. Diagrams of equivalent Von Mises stress distribution in the analyzed cross section

4 Analytical review based on the tensile test and FEA

Based on the results from the tensile test and FEA, this study proposes analysis methods in the flat beam joint subjected to tensile force as shown in Eq (4), (5), (6), (7), (8), (9) and (10).

$$P_e = 2 \cdot n \cdot e \cdot t_b \cdot {}_b\sigma_y/\sqrt{3} \tag{4}$$

In case of $L_s \geq \sqrt{3} \cdot B - e$

$$P_y = min\begin{cases} \left(0.46 \cdot {}_bA_f + 0.57 \cdot {}_bA_w\right) \cdot {}_b\sigma_y \\ \left(0.25 \cdot {}_jA_f + {}_jA_{ew}\right) \cdot {}_j\sigma_y \\ P_f \end{cases} \tag{5}$$

In case of $L_s < \sqrt{3} \cdot B - e$

$$P_y = min\begin{cases} \left(0.3 \cdot {}_bA_f + 0.57 \cdot {}_bA_w\right) \cdot {}_b\sigma_y \\ \left(0.25 \cdot {}_jA_f + {}_jA_{ew}\right) \cdot {}_j\sigma_y \\ P_f \end{cases} \tag{6}$$

$${}_jA_{ew} = min\begin{cases} 2.4 \cdot {}_jt_w^2 \cdot \sqrt{E/\,{}_j\sigma_y} \\ {}_jA_w \end{cases} \tag{7}$$

$$P_u = Max\begin{cases} 2 \cdot (k \cdot \alpha \cdot d_0 + e) \cdot t_b \cdot {}_b\sigma_u \\ 2 \cdot (L_s + e) \cdot t_b \cdot {}_b\sigma_u \qquad (L_s\text{=40mm}) \\ P_f \end{cases} \tag{8}$$

$$k = min(1.4\,h'/d_0 - 1.7,\ \ 2.5) \tag{9}$$

$$\alpha = min\left(L_s/3d_0 - 0.25,\ \ {}_bF_u/\,{}_b\sigma_u,\ \ 1.0\right) \tag{10}$$

n : total number of bolts, ${}_bt$: thickness of beam [mm], ${}_jt$: thickness of jointing parts [mm], ${}_b\sigma_y$: yield stress of beam, ${}_j\sigma_y$: yield stress of jointing parts, ${}_b\sigma_u$: tensile strength of beam, ${}_bA_f$: sectional area of beam flange, ${}_bA_w$: sectional area of beam web, ${}_jA_f$: sectional area of jointing parts flange, ${}_jA_{ew}$: effective sectional area of jointing parts web, E : young's modulus, d_0 : bolts holes diameter, ${}_bF_u$: tensile strength of bolts.

Table 6 shows theoretical values of the elastic limit strength, effective cross section yield strength and maximum strength based on the evaluation methods above.

The elastic limit strength was evaluated as the shear yield at the end opening distances. The yield strength was assessed as the minimum value of effective cross section yield of the beam or jointing parts or frictional strength. The effective cross-sectional area of the beam web and flange were appraised based on the result from the tensile test and FEA, and the jointing parts were done following the design standard for steel structures (transaction of AIJ) [3]. In case of L_s=40, the maximum strength was determined by the shear failure at the bolt bound section (L_s) and end distance (e). In the other specimens, it was evaluated as bearing failure at the force side bolts and end opening fracture at the end distance. As for bearing failure, the parameters (k, α) were based on the configuration of the test specimens [4].

Table. 6. Comparison of theoretical and experimental value

Classif-ication	Specimen Label e-t-L_s	Elastic Limit Strength P_e[kN]		Effective Cross section Yield Strength P_{ey}[kN]		Maximum Strength P_u[kN]		Collaps Process
		test	theory	test	theory	test	theory	
A	22-3.2-8	252	219	400	370	429	382	1
	22-4.5-8	89	219	374	370	447	382	2
	22-3.2-12	265	219	393	370	414	382	2
	22-4.5-12	231	219	404	370	455	382	1
B	22-3.2-40	284	219	317	322	332	349	3
	22-4.5-40	92	219	308	322	339	349	2
	28-3.2-80	373	278	-	370	426	411	4
	28-4.5-80	308	278	360	370	453	411	5
	28-3.2-90	286	278	287	370	389	411	5
	28-4.5-90	239	278	310	370	396	411	5
	28-3.2-120	243	278	404	370	407	411	5
	28-4.5-120	326	278	351	370	443	411	2

5 Conclusions

The following conclusions were drawn from this study:

(1) This study revealed the fundamental properties of the mechanical behavior and resistant mechanism of the flat joint method from the tensile test on the flat beam joint; that is, stress on the beam is transmitted to the jointing parts by way of bolts and friction force.

(2) The yield, frictional surface slipping, bearing failure and end opening fracture were observed in the tensile test. Also, dispersion in coefficient of friction affected the collapse process.

(3) Based on the results of the tensile test and FEA, we proposed the evaluation methods of the flat beam joint subjected to tensile force, which are generally consistent with the test results.

References

1. Architectural Technology (2023) The Kenchiku Gijutsu 2023 February. 1st edn. Architectural Technology Co.,Ltd, Tokyo
2. Architectural Institute of Japan (2009) Recommendations for the Design and Fabrication of Light Weight Steel Structures. 2nd edn. AIJ, Tokyo
3. AIJ (2021) AIJ Standard for Allowable Stress Design of Steel Structures. 1st edn. AIJ, Japan
4. Toda Y, Yamaguchi T, Mineyama Y and Naoe Y (2014) Experimental study of mearing strength of friction bolted connection based on bolt hole deformation. Japanese Journal of JSCE A1 70(3):333-435